

Massive droplets generation for digital PCR via a smart step emulsification chip integrated in a reaction tube

Shuhao Zhao,^a Zengming Zhang,^a Fei Hu,^a Junjun Wu,^a Niancai Peng ^{*a}

^a State Key Laboratory for Manufacturing Systems Engineering, Xi'an Jiaotong University, Xi'an, 710054, Shaanxi, China

*Corresponding author: Niancai Peng, E-mail: ncpeng@mail.xjtu.edu.cn

Supporting information

Table of Contents

Supplementary video description.....	2
Text S1. Fabrication of the SU-8 mold.....	2
Text S2. Measurement of the fluid properties	3
Text S3. PCR reagent preparation	3
Text S4. Evaluation of the droplet size distribution	5
Text S5. Droplet generation via the SE device	5
Text S6. Poisson statistics in the ddPCR tests	11
Text S7. Quantitative results in the ddPCR experiments.....	12
References.....	15

Contains

Number of pages: 15

Number of figures: 8

Number of tables: 9

Supplementary video description

Video name	Video description
SV1	Droplet generation by using step emulsification (SE) devices with different layouts of micro-channels. All of the SE devices can stably perform droplet preparation.
SV2	An integrated SE device producing monodisperse droplets with a diameter of $\sim 65 \mu\text{m}$ at a total flow rate of $10 \mu\text{L}/\text{min}$. The droplets are generated in the customized reaction tube directly with a total generation frequency of $\sim 1.1 \text{ kHz}$.
SV3	Monodisperse droplets prepared in a 2.0-mL centrifuge tube by using a compact SE chip. The chip contains 12 nozzles with a rectangular cross section of $150 \mu\text{m}$ (W) \times $28 \mu\text{m}$ (H). An electronic pipette was used to inject the aqueous solution. When the total flow rate (Q) increases from $0.5 \mu\text{L}/\text{min}$ to $50 \mu\text{L}/\text{min}$, the droplet generation frequency increases significantly with inconspicuous change in the droplet size. Video shows that the droplets leave the nozzle exits rapidly due to buoyancy.
SV4	The whole procedure of the droplet generation by using a circular SE chip integrated in a 10 mm (L) \times 10 mm (W) \times 45 mm (H) cuvette. The circular SE chip contains 24 rectangular nozzles. Monodisperse droplets are producing at a total flow rate of $20 \mu\text{L}/\text{min}$.
SV5	Removal of the pipette tip or the tiny SE chip after finishing the droplet preparation. No significant droplet loss occurred during the transferring process.

Text S1. Fabrication of the SU-8 mold

The molding master for the SE chip consists of two layers of SU-8 photoresist based on a silicon wafer. Thus the step structure at the nozzle exits can be obtained, and then the PDMS chips are cut into individual chips along the step accurately. Figure S1 shows the manufacturing process of the SU-8 molding master. Initially, a thinner layer of SU-8 photoresist is spin-coated onto the silicon wafer and exposed with a mask to obtain the mold of micro-channel structure. After developing and hard baking, a second layer of SU-8 photoresist with a thickness of several hundred microns is spin-coated onto the same wafer. With the help of the alignment mark on the silicon wafer, the mask for the second exposure is aligned with the first layer structure by using a mask aligner system (ABM, USA). Then a SU-8 mold with two layers of photoresist can be obtained. The thickness of the SU-8 photoresist changes abruptly at the nozzle exits.

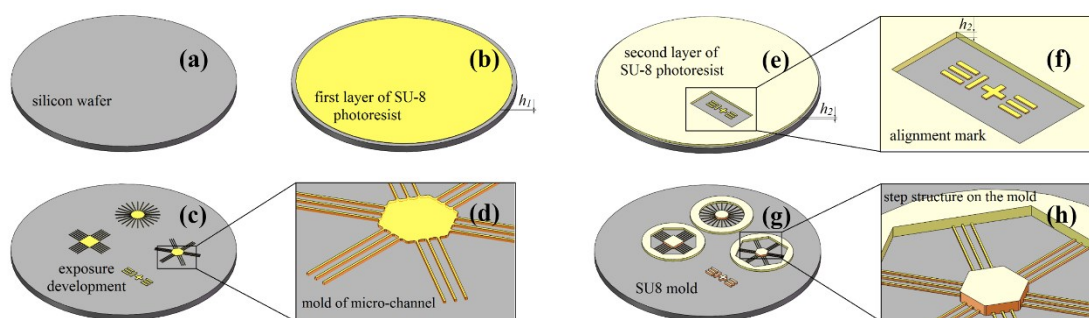


Figure S1 Manufacturing procedures of the SU-8 molding master. (a) The silicon wafer; (b) A thinner layer (h_1) of SU-8 photoresist spin-coated onto the silicon wafer; (c) Exposure and development; (d) Zoom in on the mold of the micro-channel structure; (e) The second layer (h_2) of SU-8 photoresist spin-coated onto the same silicon wafer. The area of the mark is reserved for the mask alignment; (f) Enhancement of the alignment mark; (g) The SU-8 molding master including three representative chip designs; (h) Step structure on the outer edge of the chip mold.

As shown in Figure S2, the size of the manufactured SU-8 molds are measured via the digital microscope (VHX-600, Keyence, Japan) and the optical profilometer (PGI Optics 3D, Talysurf, UK). By changing the thickness of SU-8 photoresist in the mold, several SE devices with different nozzle dimensions can be manufactured to prepare monodisperse droplets with a diameter in the 30–300 μm range.

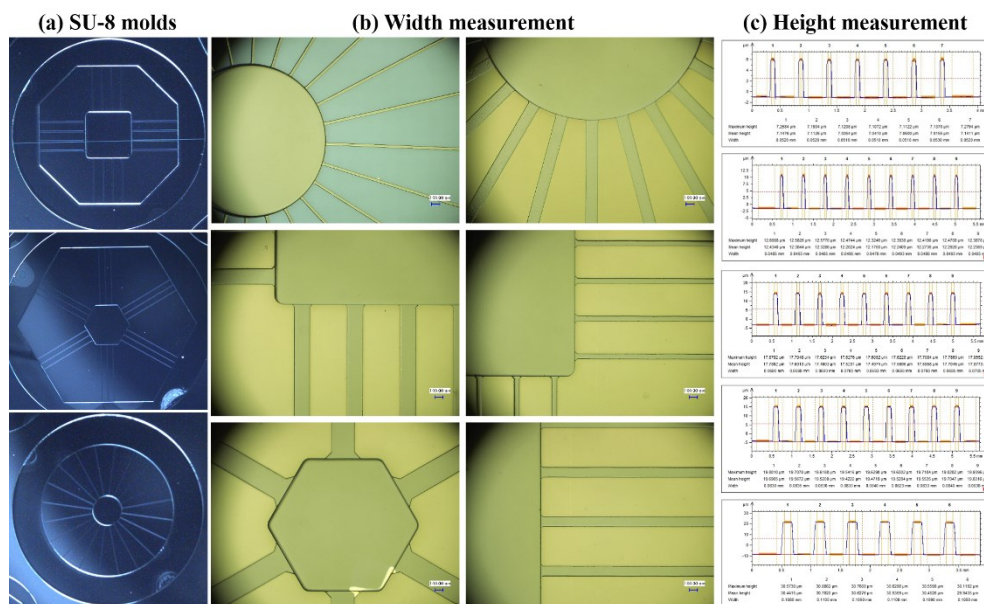


Figure S2 Measurement of the channel width and the channel height of the SU-8 mold. (a) Three representative SU-8 molds; (b) Width measuring via the digital microscope; (c) Measuring results of the height via the optical profilometer.

Text S2. Measurement of the fluid properties

The interfacial tension between two-phase fluids was measured by using a contact angle meter (JC2000D, Powereach, China) via the pendant-drop method.¹ Moreover, the viscosities of the continuous phase and the dispersed phase were tested with a digital viscometer (SNB-1, Shanghai NiRun Intelligent Technology, China). Fluid properties including the viscosities and the interfacial tensions between two-phase fluids were measured at 20 °C – the temperature in which the experiment of the droplet generation was conducted.

Table S1. Measurement of the fluid properties

Dispersed phase	Density, ρ_{dis}	Viscosity, μ_{dis}	Continuous phase	Density, ρ_{con}	Viscosity, μ_{con}	Surface tension of the Continuous phase, σ_{con}	Interfacial tension, γ
/	[g/cm ³]	[mPa·s]	/	[g/cm ³]	[mPa·s]	[mN/m]	[mN/m]
PCR buffer (1×)	1.0	1.4	Novec HFE-7500 oil supplemented with 2.0% w/w PFPE ₂ -PEG	1.6	1.3	16	8±1

Text S3. PCR reagent preparation

The sequences of primers, probe and DNA template are listed in Table S2. The primary DNA concentration was roughly assessed via UV-spectrophotometry (NanoDrop 2000, ThermoFisher Scientific, USA). Then, serial dilution was performed to obtain a series of DNA samples with different template concentrations.

Table S2. Oligo DNA sequences

Oligo-DNAs	Sequence
EGFR T790M mutation (DNA template), 270 bp	5'-ATGTGCCCTCCTTCTGGCCACCATGCGAAGCCACACTGACGTGCCTCTC CCTCCCTCCAGGAAGCCTACGTGATGGCCAGCGTGGACAACCCCCACGTGT GCCGCCTGCTGGGCATCTGCCTCACCTCCACCGTGCAGCTCATCATGCAGC TCATGCCCTTCGGCTGCCTCCTGGACTATGTCCGGGAACACAAAGACAATA TTGGCTCCCAGTACCTGCTCAACTGGTGTGTGCAGATCGCAAAGGTAATCA GGGAAGGGAGATACGGGGAGGGGAGATAAGG
Forward primer	5'-GCCTGCTGGGCATCTG-3' (162058)
Reverse primer	5'-TCTTTGTGTTCCCGGACATAGTC-3' (162152)
TaqMan probe for T790M mutation	5'-FAM-ATGAGCTGCATGATGAG-MGB-NFQ-3'.
Amplicon sequence, 95 bp	5'-GCCTGCTGGGCATCTGCCTCACCTCCACCGTGCAGCTCATCATGCAGCTC ATGCCCTTCGGCTGCCTCCTGGACTATGTCCGGGAACACAAAGA-3' (EGFR gene, GRCh38.p12)

The PCR reagents used in ddPCR tests mainly consist of the following components: PCR Mixture (2×), DNA polymerase, primers, probe, and DNA template. The PCR reaction components are stored at -20 °C prior to their use and premixed before starting the droplet preparation process. Nuclease free water (ThermoFisher Scientific, USA) is used to prepare the PCR reagent. Emulsions prepared via the SE device use the proprietary products from Xi'an Tianlong Technologies as the aqueous solution. As a comparison, commercial reagents from Bio-Rad are used to prepare emulsions via the commercial QX200 Droplet Generator (QX200 DG). The recipes of PCR reagent are listed in Table S3–S4.

Table S3. Recipe of the PCR reagent for QX200 DG

For 20 µL/Sample	Vol. /µL	Stock Concentration	Final Concentration
ddPCR Supermix for Probes (containing DNA polymerase, dNTPs)	10	2×	1×
Forward Primer	1	10 µM	0.5 µM
Reverse Primer	1	10 µM	0.5 µM
TaqMan Probe	1	5 µM	0.25 µM
DNA template	2	--	--
Nuclease free water	5	--	--
Total volume	20	--	--

Table S4. Recipe of the PCR reagent for the SE device

For 20 µL/Sample	Vol. /µL	Stock Concentration	Final Concentration
PCR Master Mix (containing dNTPs)	10	2×	1×
DNA Polymerase	0.5	5 U/µL	0.125 U/µL
Forward Primer	1	10 µM	0.5 µM
Reverse Primer	1	10 µM	0.5 µM
TaqMan Probe	1	5 µM	0.25 µM
DNA template	2	--	--
Nuclease free water	4.5	--	--
Total volume	20	--	--

Text S4. Evaluation of the droplet size distribution

A single layer of droplets was prepared for the microscopic observation. Photographs of droplets were taken using a digital color camera (DFC310FX, Leica Microsystems Inc., Germany) and Leica Application Suite software (Leica Microsystems Inc.). Then the images were analysed with the ImageJ software to obtain the size and the uniformity of the droplets. As shown in Figure S3, droplets with three different diameters prepared by the SE devices were used as cases for analysis.

The mean diameter of the droplets (\bar{d}) was calculated using:

$$\bar{d} = \sum_{i=1}^n d_i / n$$

where n is the number of droplets observed and d_i is the diameter of a droplet. The coefficient of variation (CV) of droplet diameter was calculated as:

$$CV = (\sigma / \bar{d}) \times 100\%$$

where σ is the standard deviation of the droplet diameters.

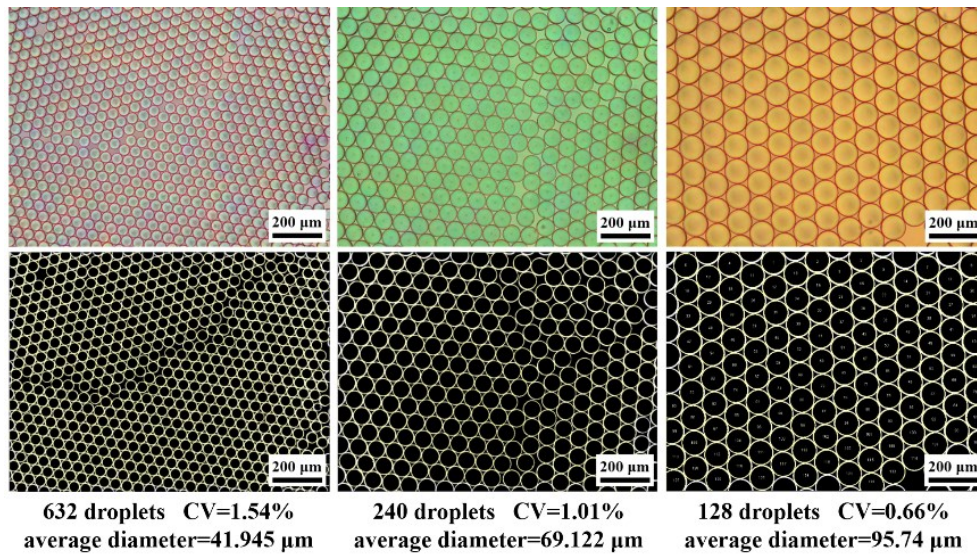


Figure S3 Evaluation of the droplet size distribution by using the ImageJ software. Top: Droplet images taken by an optical microscope; Bottom: The circumferences of the droplets are identified and then the fitted dropltes are labeled in yellow.

Text S5. Droplet generation via the SE device

As shown in Figure S4a and S4b, the w/o droplets floated on top of the emulsion due to buoyancy, and then closely packed on the upper layer of the oil phase. According to the value for the density of random close packing of equal spheres provided by previous studies,^{2,3} the volume fraction of the aqueous solution in the supernatant emulsion can reach to ~64%. In addition, droplet deformation caused by its buoyancy can further increase the value of droplet packing density. Therefore, for a SE device with a certain size, the amount of two-phase fluids in a single droplet preparation can be calculated. In order to reduce the impact of the SE chip on the w/o droplets in subsequent PCR amplification, a certain space ($\Delta H = H_1 - H_2$) will be reserved between the supernatant emulsion and the SE chip (Figure S4c). Thus the total volume of the fluorinated oil (V_{oil}) can be calculated by

$$V_{oil} = V_{bottom} + V_{oil_sup} ,$$

$$V_{bottom} = \pi(D_1^2 \times H_1 - D_2^2 \times H_2) / 4 ,$$

$$V_{\text{oil_sup}} = (1 - 0.64) \times V_{\text{dis}} / 0.64,$$

V_{bottom} refers to the volume of the pure oil in the bottom of the reaction tube, $V_{\text{oil_sup}}$ is the volume of the oil in the supernatant emulsion, V_{dis} is the volume of the disperse phase in the supernatant emulsion.

By optimizing the size of the overall SE device, for example, $D_1=8$ mm, $D_2=6$ mm, $H_1=3.0$ mm and $H_2=2.5$ mm, droplet preparation with 100 μL of aqueous solution will require ~ 136 μL of the fluorinated oil. Furthermore, when the SE chip is small enough, it can be used in combination with a 0.2-mL centrifuge tube. The chip nozzle could be dipped into the continuous phase by adding 45 μL of the fluorinated oil (Figure S4d). By calculation, it can be known that the stable droplet preparation of 50 μL of aqueous solution can be completed with ~ 75 μL of oil phase, which is very suitable for ddPCR analysis.

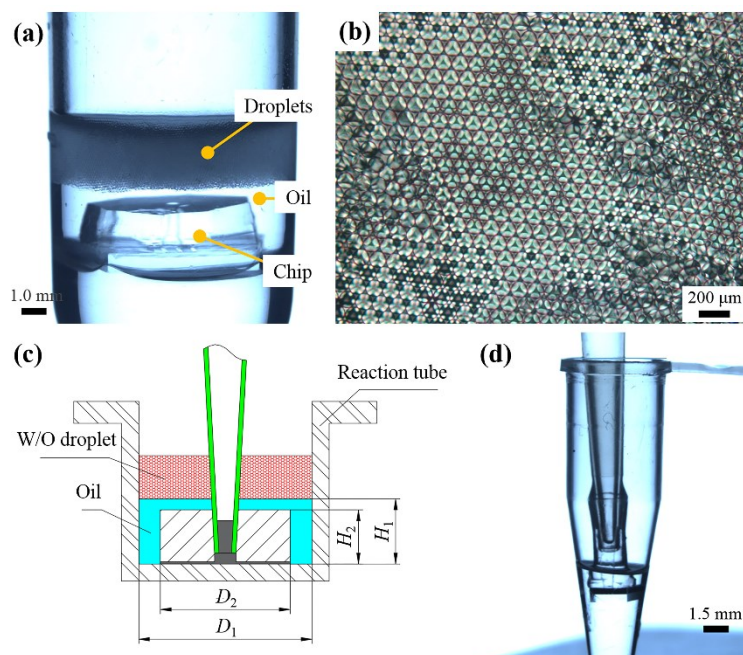


Figure S4 Droplet generation via the SE device. (a) Droplet preparation in a 2.0-mL centrifuge tube. The bottom of the centrifuge tube was filled with cured PDMS. After preloading 300 μL of the fluorinated oil, 200 μL of aqueous solution was dispersed into monodisperse droplets; (b) Microscopic observation of the closely packed droplets; (c) Schematic diagram of the SE device with an optimized design. To simplify the calculation of reagent volume, both the SE chip and the reaction tube are cylindrical; (d) A tiny SE chip assembled with 0.2-mL centrifuge tube. 45 μL of the oil phase was added to the centrifuge tube.

PCR buffer (1 \times) and Novec HFE7500 supplemented with fluoro-surfactant were used as the disperse phase and the continuous phase, respectively. As shown in Table S5 and Figure S5, a SE device equipped with 12 nozzles was used to generate droplets under different flow rates. Each nozzle has a rectangular cross section of 150 μm (W) \times 28 μm (H). The average droplet generation frequency per nozzle (f_a) was estimated as:

$$f_a = \frac{Q_a}{\bar{v}}$$

In this expression, Q_a corresponds to the average flow rate of the disperse phase per nozzle, \bar{v} refers to the average volume of the droplet which was calculated using:

$$\bar{v} = \frac{\pi \bar{d}^3}{6}$$

where \bar{d} is the mean diameter of the droplets.

Table S5. Droplet generation under different average nozzle flow rates (Q_a)

Q_a	\bar{d}	Standard deviation of \bar{d}	CV of \bar{d}	f_a	Numbers of droplets analysed
[$\mu\text{L}/\text{min}$]	[μm]	[μm]	/	[Hz]	/
0.10	94.91	1.52	1.81%	3.72	403
0.50	95.37	1.22	1.38%	18.35	638
1.00	96.30	0.91	1.05%	35.64	637
2.25	99.07	0.65	1.32%	73.66	558
3.00	100.92	0.95	1.88%	92.91	538
5.00	106.94	0.72	1.34%	130.14	439
7.50	112.96	0.66	0.58%	165.63	428
8.50	115.74	0.75	0.65%	174.51	450
8.75	116.67	0.85	0.73%	175.38	447
9.00	425.92	5.93	1.39%	3.71	29
9.50	450.00	6.34	1.41%	3.32	24
10.00	462.96	9.34	2.02%	3.21	27

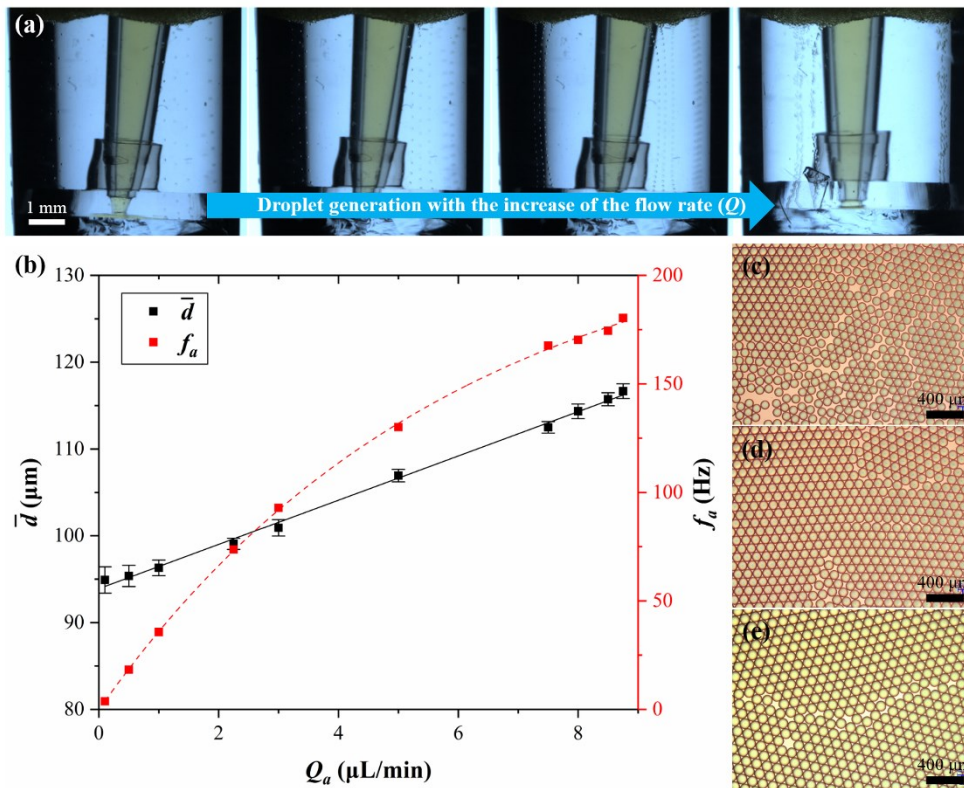


Figure S5 Droplets generation under different flow rates. A compact SE chip equipped with nozzle dimensions of $150\ \mu\text{m}$ (W) \times $28\ \mu\text{m}$ (H) was used in this test. (a) Droplets generation with the increase of the flow rate. An electronic pipette were used to complete the injection of the aqueous solution. As the total flow rate increases, the droplet generation frequency increases significantly with inconspicuous change in the droplet size; (b) Influence of the average nozzle flow rate (Q_a) on the average droplet diameter (\bar{d}) and on the average generation frequency per nozzle (f_a). The total flow rate of the PCR buffer (Q) of was precisely controlled by a syringe pump. In dripping regime, the average droplet diameter exhibits a slight growth ($< 25\%$) and remains monodisperse with a CV $< 2.0\%$. The value of the droplet generation frequency increases rapidly with the increase of Q_a . Error bars represent the standard deviations of droplet diameter; (c, d, e) Images of monodisperse droplets prepared at average nozzle flow rates of $1.0\ \mu\text{L}/\text{min}$, $3.0\ \mu\text{L}/\text{min}$ and $8.5\ \mu\text{L}/\text{min}$, respectively.

By using SE devices with the cross section of the nozzles with a width-to-height ratio (WHR) of 5–6, the relation

between the maximum production rate per nozzle (Q_a^*) and the nozzle height (H) are explored. The measuring results are listed in Table S6. In addition, the diameters of droplets prepared by these SE devices were investigated under three flow conditions of Q_a^* (\blacksquare), $Q_a^*/2$ (\otimes), and $Q_a^*/10$ (\bullet), respectively.

Table S6. Maximum production rates per nozzle and the critical Capillary number of the disperse phase measured in each device

Nozzle Height (H)	Nozzle Width (W)	Numbers of Nozzles	Q^* for the PCR Buffer	Q_a^* for the PCR Buffer	U_{buf}^*	Ca^*
[μm]	[μm]	/	[$\mu\text{L}/\text{min}$]	[$\mu\text{L}/\text{min}$]	[m/s]	/
8	40	18	12	0.67	0.0349	0.00611
18	100	20	75	3.75	0.0347	0.00608
28	150	12	105	8.75	0.0347	0.00608
37	200	12	180	15.0	0.0338	0.00591
60	310	6	230	38.33	0.0344	0.00601
68	400	6	330	55	0.0337	0.00590
Sum	/	/	/	/	0.0344 ± 0.0005	0.00601 ± 0.00008

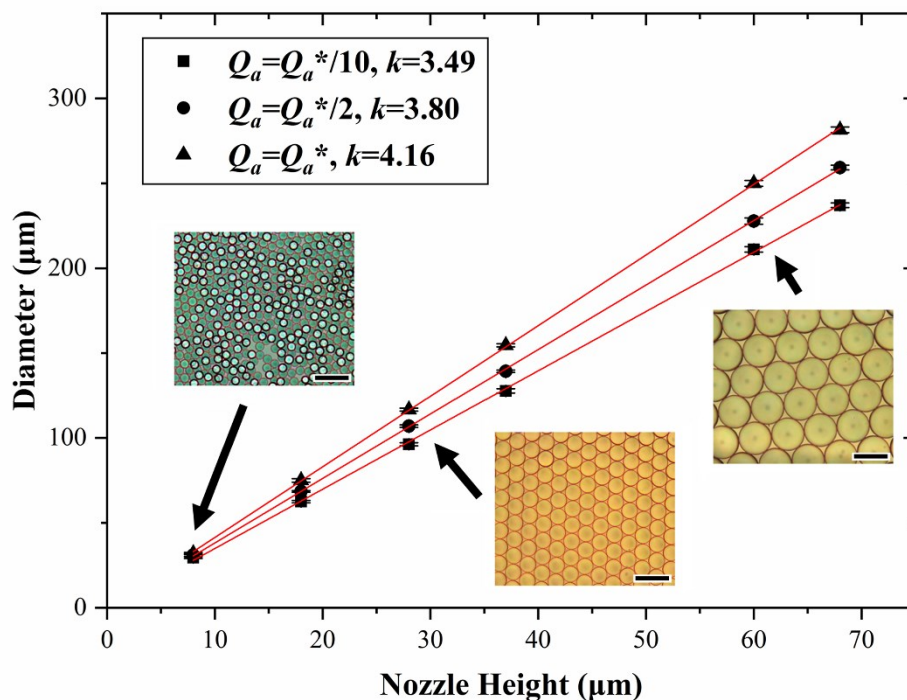


Figure S6 Linear relation between the droplet diameter and the nozzle height for the SE devices. For each SE device with a nozzle height in the 5–70 μm range, droplets diameter were investigated under three flow conditions of Q_a^* (\blacksquare), $Q_a^*/2$ (\otimes), and $Q_a^*/10$ (\bullet), respectively. The Q_a^* value corresponds to the maximum production rate per nozzle to obtain monodisperse droplets for each device. The slope factors of the three linear fitting lines are 3.49 (\bullet), 3.80 (\otimes), and 4.16 (\blacksquare), respectively. Error bars are the standard deviations of droplet diameter. The scale bar measures 200 μm .

As shown in Figure S7, SE chip with dimensions of 2.0 mm (L) \times 2.0 mm (W) \times 0.9 mm (H) has been manufactured

by using silicon based MEMS processing technologies. The entire fabrication process includes repeated plasma etching of silicon wafer, anodic bonding between the silicon wafer and the glass wafer, wafer dicing, and vapor deposition of hydrophobic coating. A piece of silicone tube is used as a connector to connect the tiny SE chip to the pipette tip, and it can later be replaced with a customized injection molded part.

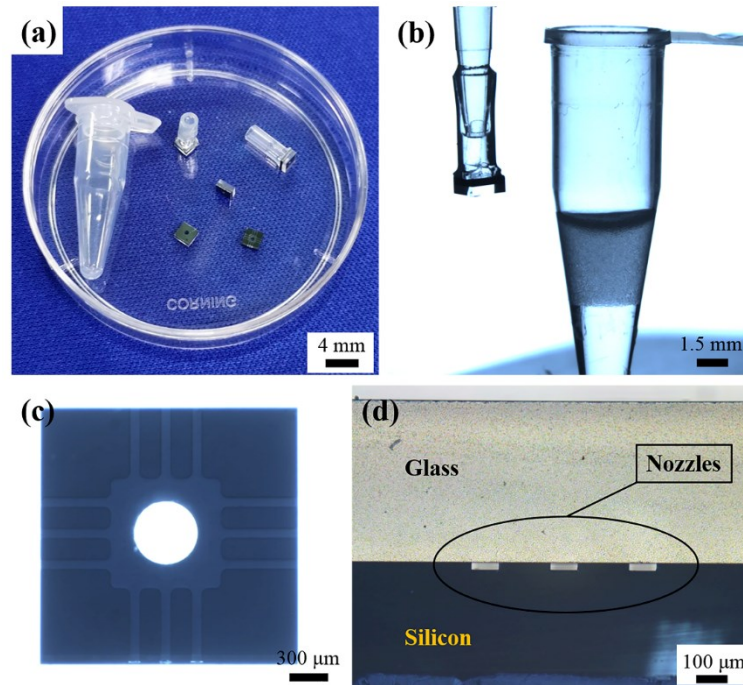


Figure S7 Mass production and industrialization of the SE chip. (a) The morphology and size of the tiny SE chip. SE chip with dimensions of 2.0 mm (L) \times 2.0 mm (W) \times 0.9 mm (H) has been manufactured with materials of silicon and glass. A short piece of silicone tube is fixed at the chip inlet as a connector; (b) Droplet preparation via the smart SE tip. The chip can be directly connected to the pipette tip, and then used in combination with a 0.2-mL centrifuge tube; (c) Microscopic observation of the micro-channels in the SE chip; (d) Microscopic observation of the chip sidewall. The rectangular nozzles have uniform size.

Table S7 Comparison of different ddPCR platforms⁴

Platforms Characteristics	Bio-Rad QX200 ddPCR System⁵	RainDance Technologies RainDrop System	Stilla Technologies Naica System⁶	Centrifugal Step Emulsification⁷	MiCA⁸	Our Design
Droplet generation method	Flow focusing	Flow focusing	SE with confinement gradients	Centrifugal step emulsification	Centrifugal micro-channel array in a reaction tube	Compact SE in a reaction tube
Droplet diameter (Volume)	~118 μm (0.85 nL ⁹)	~21 μm (5 pL)	94 μm (0.43 nL)	147 μm (1.8 nL)	50 μm (0.065nL)	101.5 μm (0.55 nL) and 65 μm (0.14 nL)
Number of droplets per sample	20 000 (Ideally) ~15, 000 (Tested)	5–10 million (Ideally)	2.5–3.0 $\times 10^4$	~11 000 (Ideally)	~3.0 $\times 10^5$ (Ideally) ~2.5 $\times 10^5$ (Tested)	Adjustable, 2.5–2.7 $\times 10^4$ droplets with a volume of 0.55 nL were detected for 20 μL of PCR reagent
Volume of PCR reagent per sample	20 μL	25–50 μL	25 μL	20 μL	20 μL	20–50 μL
Time for droplet generation	<2 min	~30 min for 25 μL PCR reagent	~10 min	8 min	< 7 min	< 2 min for 50 μL PCR reagent
Thermocycling	Performed in a 96-well plate	Performed in a 8-tube Strips	Performed in a thin chamber accompanied by overpressure	Performed in a tapered chamber	Performed in a centrifuge tube	Performed in a reaction tube

Text S6. Poisson statistics in the ddPCR tests

The PCR reagent including m copies of DNA template is divided into massive monodisperse droplets in ddPCR test. The dispersion of DNA template in the droplets conforms to the Poisson distribution.^{10,11}

The total number of the droplets (N) can be calculated by the equation:

$$N = \frac{V}{\bar{v}}$$

In this expression, V is the total volume of the PCR reagent in each test, \bar{v} refers to the average volume of the droplets. Then the average copies of DNA template in one droplet is defined as,

$$\lambda = \frac{m}{N}$$

Thus the template concentration

$$C = \frac{m}{V} = \frac{\lambda}{(V/N)} = \frac{\lambda}{\bar{v}}$$

According to the Poisson distribution, when N is large enough, the probability of containing at least one copy of DNA template in a given droplet is

$$p = 1 - e^{-\lambda}$$

Therefore,

$$\lambda = -\ln(1-p)$$

In the ddPCR experiments, the droplets containing at least one copy of DNA template exhibit a positive signal after the PCR amplification process. The number of positive droplets (a) and the number of negative droplets (b) can be obtained by reading their fluorescence intensity. Since tens of thousands of droplets are analysed in each ddPCR test, and the detection ratios of the effective droplets exceeds 70%, it can be estimated that

$$\hat{p} = \frac{a}{a+b} = 1 - \frac{b}{a+b},$$

where \hat{p} is an unbiased estimator of p . The standard deviation of \hat{p} for large N is calculated by

$$\sigma = \sqrt{\frac{(1-p)p}{N}}$$

Then the lower and upper confidence limits (\hat{p}_L, \hat{p}_H) are approximately calculated by

$$\hat{p}_{L,H} = \hat{p} \pm Z_c \times \sigma$$

The estimator of λ is defined as

$$\hat{\lambda} = -\ln(1-\hat{p}) = -\ln\left(\frac{b}{a+b}\right)$$

Since the droplets are monodisperse in digital PCR, the DNA concentration can be calculated as

$$\hat{C} = \frac{\hat{\lambda}}{\bar{v}} = -\ln\left(\frac{b}{a+b}\right) \frac{1}{\bar{v}}$$

For 95% confidence level, $Z_c=1.96$. Thus,

$$\hat{p}_{L,H} = \hat{p} \pm 1.96 \times \sqrt{\frac{(1-\hat{p})\hat{p}}{N}}$$

And the confidence interval [$\hat{\lambda}_L, \hat{\lambda}_H$] at the 95% confidence level is given as follows

$$\hat{\lambda}_L = -\ln(1 - \hat{p}_L) \text{ and } \hat{\lambda}_H = -\ln(1 - \hat{p}_H).$$

The lower and upper confidence limits of the concentration (\hat{C}_L, \hat{C}_H) at the 95% confidence level are calculated by

$$\hat{C}_L = \frac{\hat{\lambda}_L}{\bar{v}} \text{ and } \hat{C}_H = \frac{\hat{\lambda}_H}{\bar{v}}.$$

Text S7. Quantitative results in the ddPCR experiments

After the PCR amplification process, the fluorescence distribution of the droplets in each ddPCR test can be obtained via the QX200 Droplet Reader (Bio-Rad). Raw-data was exported from QuantaSoft software. The QuantaSoft software utilized a droplet volume of 0.85 nL incorporated in the calculations. Since droplets generated by the SE devices have different sizes with that of the QX200 DG, the quantitative results were recalculated based on the principle of the Poisson statistics in Text S6.

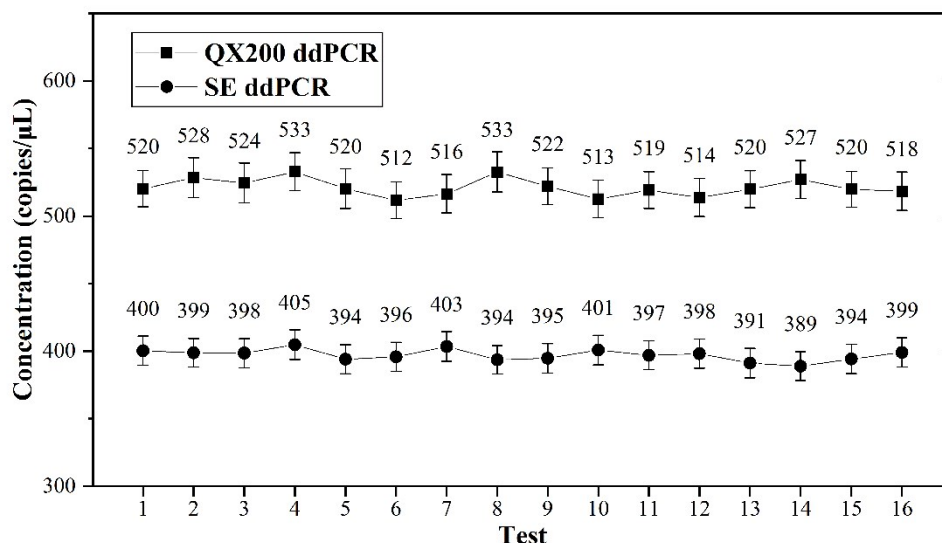


Figure S8 Repeated trials performed by using droplets prepared by the SE device and the QX200 DG. PCR reagents with two different DNA concentrations were used in the experiments, and each sample was tested 16 times. The combined quantitative results obtained from the QX200 DG (●) and the SE device (◻) are 521 ± 6.1 copies/μL and 397 ± 4.1 copies/μL. Part of the raw-data for the repeated ddPCR tests were provided in Table S8.

Table S8 listed the 8 sets of raw-data for the repeated ddPCR tests. The quantitative results exhibit good repeatability by using droplets prepared via either the SE device or the QX200 DG.

Table S8. The raw-data for the repeated ddPCR tests

Test	V	\bar{v}	N	a	b	p	λ	C	C (95% CI)*
/	[μL]	[nL]	/	/	/	[%]	/	[cp/ μL]	[cp/ μL]
QX200	repeated trials, 8 sets of raw-data								
T-1-1	20	0.85	16535	10626	5909	35.74	0.4422	520	[506,534]
T-1-2	20	0.85	13822	8821	5001	36.18	0.4491	528	[514,543]
T-1-3	20	0.85	13826	8853	4973	35.97	0.4458	524	[510,539]
T-1-4	20	0.85	15480	9842	5638	36.42	0.4529	533	[519,547]
T-1-5	20	0.85	13797	8866	4931	35.74	0.4422	520	[506,535]
T-1-6	20	0.85	15759	10201	5558	35.27	0.4349	512	[498,525]
T-1-7	20	0.85	14621	9426	5195	35.53	0.4390	516	[502,531]
T-1-8	20	0.85	13736	8735	5001	36.41	0.4527	533	[518,548]
SE	repeated trials, 8 sets of raw-data								
T-2-1	20	0.55	26502	21265	5237	19.76	0.2202	400	[389,411]
T-2-2	20	0.55	27799	22325	5474	19.69	0.2193	399	[388,409]
T-2-3	20	0.55	27151	21808	5343	19.68	0.2191	398	[388,409]
T-2-4	20	0.55	26940	21631	5309	19.71	0.2195	399	[388,410]
T-2-5	20	0.55	26653	21460	5193	19.48	0.2167	394	[383,405]
T-2-6	20	0.55	26751	21518	5233	19.56	0.2177	396	[385,406]
T-2-7	20	0.55	27839	22421	5418	19.46	0.2164	394	[383,404]
T-2-8	20	0.55	26199	21087	5112	19.51	0.2171	395	[384,406]

* C (95% CI) represents the confidence interval of the DNA concentration at the Poisson 95% confidence level.

Table S9 listed the raw-data for the ddPCR tests with adjustable volume of PCR reagents. By using the SE device, PCR reagents with a volume of 20–50 μL were converted into monodisperse droplets and utilized for the ddPCR quantitative detection. Meanwhile, droplets prepared by the QX200 DG were used as a control, and 20 μL of PCR reagent was used in each dPCR test. Samples with two different DNA concentrations obtained by 10-fold serial dilution were used for the ddPCR quantitative analysis.

Table S9 Raw-data for the ddPCR tests with adjustable volume of PCR reagents

Test	V	\bar{v}	N	a	b	p	λ	C	C (95% CI)	$(C_H-C_L)/C$ #
/	[μL]	[nL]	/	/	/	[%]	/	[cp/ μL]	[cp/ μL]	[%]
SE	ddPCR with 20–50 μL of PCR reagents									
T-3-1	20	0.55	25029	24275	754	3.01	0.0306	55.6	[51.6, 59.6]	14.39
T-3-2	30	0.55	38317	36709	1108	2.93	0.0297	54.1	[50.9, 57.2]	11.65
T-3-3	40	0.55	49844	48362	1482	2.97	0.0302	54.9	[52.1, 57.7]	10.20
T-3-4	50	0.55	63346	61445	1901	3.00	0.0305	55.4	[52.9, 57.9]	9.03
T-3-5	20	0.55	25391	18641	6750	26.58	0.309	562	[548, 575]	4.80
T-3-6	30	0.55	37935	27956	9979	26.31	0.3052	555	[544, 566]	3.96
T-3-7	40	0.55	50416	37113	13303	26.39	0.3063	557	[548, 566]	3.23
T-3-8	50	0.55	63837	46921	16916	26.50	0.3079	560	[551, 568]	3.04
QX200	Control-experiments									
T-4-1	20	0.85	14035	13424	611	4.35	0.0445	52.4	[48.2, 56.5]	15.84
T-4-2	20	0.85	12925	12378	547	4.23	0.0432	50.9	[46.6, 55.1]	16.70
T-4-3	20	0.85	13454	12880	574	4.27	0.0436	51.3	[47.1, 55.5]	16.37
T-4-4	20	0.85	14417	13795	622	4.31	0.0441	51.9	[47.8, 56]	15.80
T-4-5*	20	0.85	16535	10626	5909	35.74	0.4422	520	[506, 534]	5.38
T-4-6*	20	0.85	13822	8821	5001	36.18	0.4491	528	[514, 543]	5.50
T-4-7*	20	0.85	13826	8853	4973	35.97	0.4458	524	[510, 539]	5.53
T-4-8*	20	0.85	15480	9842	5638	36.42	0.4529	533	[519, 547]	5.25

C_L and C_H represent the lower and upper confidence limits of the concentration at the Poisson 95% confidence level.

* The raw-data is identical to the first four sets of raw-data in Table S8.

References

- 1 C. E. Stauffer, *J. Phys. Chem.*, 1965, **69**, 1933-1938.
- 2 W. S. Jodrey and E. M. Tory, *Phys. Rev. A*, 1985, **32**, 2347-2351.
- 3 G. D. Scott and D. M. Kilgour, *J. Phys. D: Appl. Phys.*, 1969, **2**, 863-866.
- 4 S. Rutsaert, K. Bosman, W. Trypsteen, M. Nijhuis and L. Vandekerckhove, *Retrovirology*, 2018, **15**, 1-8.
- 5 B. J. Hindson, K. Ness, D. A. Masquelier, P. Belgrader, N. J. Heredia, A. J. Makarewicz, I. J. Bright, M. Y. Lucero, A. L. Hiddessen and T. C. Legler, *Anal. Chem.*, 2011, **83**, 8604-8610.
- 6 J. Madic, A. Zocevic, V. Senlis, E. Fradet, B. G. Andre, S. Muller, R. Dangla and M. Droniou, *Biomolecular Detection and Quantification*, 2016, **10**, 34-46.
- 7 F. Schuler, M. Trotter, M. Geltman, F. Schwemmer, S. Wadle, E. Domínguez-Garrido, M. López, C. Cervera-Acedo, P. Santibáñez and F. von Stetten, *Lab Chip*, 2016, **16**, 208-216.
- 8 Z. Chen, P. Liao, F. Zhang, M. Jiang, Y. Zhu and Y. Huang, *Lab Chip*, 2017, **17**, 235-240.
- 9 A. B. Kosir, C. Divieto, J. Pavsic, S. Pavarelli, D. Dobnik, T. Dreo, R. Bellotti, M. P. Sassi and J. Žel, *Anal. Bioanal. Chem.*, 2017, **409**, 6689-6697.
- 10 S. Dube, J. Qin and R. Ramakrishnan, *PLoS One*, 2008, **3**, e2876.
- 11 J. F. Huggett, C. A. Foy, V. Benes, K. R. Emslie, J. A. Garson, R. J. Haynes, J. Hellemans, M. Kubista, R. Mueller and T. Nolan, *Clin. Chem.*, 2013, **59**, 892-902.